Effect of Treatment for Abandoned DBS Leads on RF-Induced Heating during 1.5T MRI

Ran Guo[#1], Wei Hu[#2], Jianfeng Zheng[#3], Caleb J Ballard[#4], Daniel Herrera[#5], Efie Mavraki[*6], and Ji Chen[#7]
[#]University of Houston, Houston, USA
[*]Aleva Neurotherapeutics SA, EPFL Innovation Park, Bâtiment D, 1015 Lausanne, Switzerland
[1]rguo3@central.uh.edu, [2]whu6@central.uh.edu, [3]jzheng4@central.uh.edu, [4]cjballar@cougarnet.uh.edu, [5]dherrer8@cougarnet.uh.edu, [6]efie.mavraki@aleva-neuro.com, [7]jchen18@uh.edu

***Abstract*—The 1.5T MRI RF-induced heating for an abandoned commercial DBS lead is evaluated in this study with two different treatment at the proximal end. The capped-end or bared-end treatment on the proximal end can change the electromagnetic model of the DBS lead at 1.5T. During the ASTM phantom testing, the abandoned lead with capped-end treatment has a significantly higher temperature rise than the same abandoned leads with bared-end treatment, however, such difference is reduced during the *in-vivo* modeling study.**

***Keywords*—RF-induced heating, DBS, abandoned lead.**

I. Introduction

The patients with active implantable medical devices (AIMDs) may be precluded from the Magnetic Resonance Imaging (MRI) scan, due to the radiofrequency (RF)-induced heating hazards caused by the interaction between the AIMD and RF field. To examine the RF-induced heating hazards for AIMD in the patient body, the validated electromagnetic model (EM) of AIMD should be developed and combined with the incident RF field in the patient body to calculate the temperature increment as described in TS/ISO 10974 [1]-[2]. For the abandoned AIMD, however, the EM model can be changed which could cause unknown risks to patients [3].

A typical DBS system consists of a leads body, an extension of the leads body, and an implantable pulse generator (IPG). However, due to patient clinical needs, the IPG and the extension may need to be removed and only the leads body would remain inside the body. The leads body remained inside the human body is often referred as an abandoned lead. The proximal end of the abandoned leads body can be capped with insulator (capped-end treatment) or making direct contact with tissue (bared-end treatment). Previous studies have shown that the abandoned pacemaker leads can change the RF-induced heating for nearby intact pacemaker systems [4]. The different treatments on abandoned pacemaker leads could cause large variations of the RF-induced heating for nearby pacemaker systems up to 65%. It was also observed that the RF-induced heating is affected by the input impedance of an AIMD [5]. Hence, the treatment impact on the RF-induced heating of abandoned leads needs a comprehensive study and analysis.

In this study, the RF-induced heating of an abandoned commercial DBS system with either bared-end or capped-end treatment at the connector is measured inside the American Society for Testing and Materials (ASTM) phantom [6] and evaluated in a virtual adult male model [7]. It is shown that the validated EM models, namely transfer functions (TFs), can be changed with different proximal end treatments. Although the DBS lead with capped-end treatment has a much higher temperature rise than the one with bared-end configuration in phantom, this difference is reduced for the *in-vivo* environment.

II. Method

The RF-induced heating for a DBS system and its abandoned leads were evaluated in two different surrounding media. Overall, the RF-induced heating was evaluated under four configurations, 1) at the distal end of the original intact DBS system (the stimulation leads, the leads extension, and the IPG), 2) at the distal end of the abandoned leads with capped-end treatment, 3) at the distal end of the abandoned leads with bared-end treatment, and 4) at the proximal end of the abandoned leads with bared-end treatment. The two media have electrical conductivity of 0.47 S/m and 0.20 S/m. These two values were used based on the human body averaged conductivity value and averaged conductivity value in the DBS implanted region.

The process of heating evaluation started with the measurement of the transfer function. The TF was measured with a straight-line geometry based on the reciprocity method in a homogenous ASTM phantom. For the abandoned leads, the current probe measured the induced current along the entire leads body at 0.5 cm resolution. The predicted temperature rise using the values of the electric field strength and the measured TF were both then inputted into equation:

$$\Delta T_{tip} = A \times \left| \int TF(l) E_{tan}(l) dl \right|^2 \quad (1)$$

where A is the scaling coefficient to be determined.

To obtain the scaling coefficient A for the transfer function models, the temperature rises of all cases cases were measured along nine different lead pathways inside the ASTM phantom under the MR RF coil emissions. Three of these pathways are L-shaped, three are U-shaped, and the remaining three are straight pathways parallel along the ASTM phantom sidewall as shown in Fig. 1. Each straight, U-shaped, and L-shaped pathway were positioned with distances 2 cm, 6 cm, and 8 cm from the left sidewall of the phantom box. Once the lead was in the right position, the phantom box was placed at the center of the RF-coil. The RF-induced heating was then measured to obtain the scaling coefficient and for the transfer function model validation.

The *in-vivo* RF-induced heating is also evaluated with equation (1). The numerical simulations are conducted using the full-wave EM simulation software SEMCAD X 14.8.6

(SPEAG, Zurich, Switzerland). The adult male model (Duke, 34 years, BMI 22.4) from the Virtual Population is used for the trajectory development as well as the numerical simulation, as shown in Fig. 2. In total, different trajectories and landmark positions are considered in this study. The incident RF field is generated with a generic RF birdcage coil (diameter of 63 cm and a length of 65 mm) operating at 64 MHz (1.5T). The circular polarized RF field is generated inside the RF coil. The tangential electric fields along each clinically relevant trajectory are numerically calculated and extracted under the limits of the Normal Operating Mode with the whole-body averaged SAR of 2 W/kg or the head averaged SAR of 3.2 W/kg.

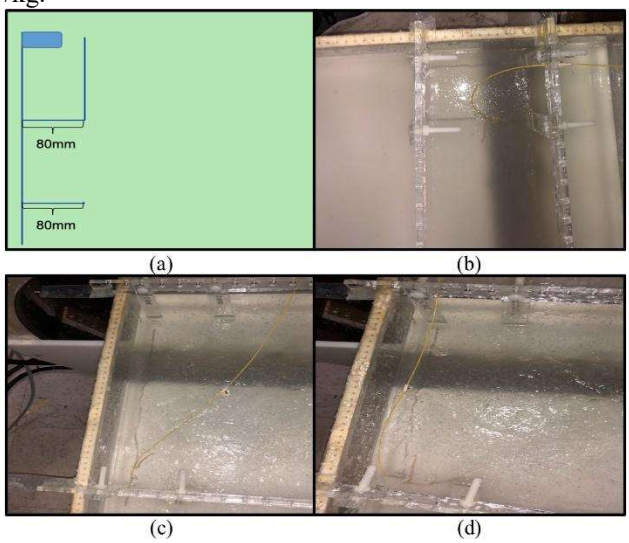

Fig. 1. (a) Three different pathways: Straight, L-shape, U-Shape. Simulation of the (b) U-Shape, (c) straight, and (d) L-Shape pathway 2 cm away from the edge.

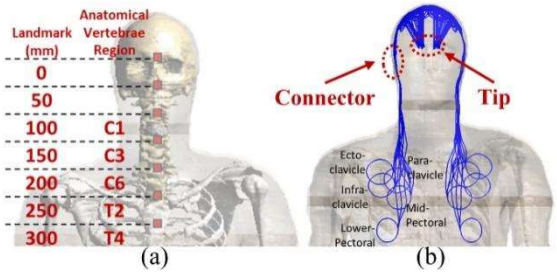

Fig. 2. (a) Illustration and landmark positions of the adult male model. (b) Developed lead trajectories of the DBS system with marked tip and connector positions.

III. Results

To study the RF-induced heating for abandoned leads, the direct measurement comparison for the three cases (configurations 2-4) are given in Table 1 and Table 2 for medium 0.47 S/m and 0.2 S/m. When comparing all nine pathways in each test case, the experiment with the leads that has capped-end treatment shown to have the highest measured change in temperature since the energy cannot be dissipated into the surrounding gel at the proximal end. In all three cases, the U-shaped layout had lower in temperature rises. This is due to the field cancellation.

Table 1. Measured temperature (°C) in medium 0.47 S/m.

	S1	S2	S3	L1	L2	L3	U1	U2	U3
Distal end heating with bared-end treatment	10.8	8.0	4.6	8.9	4.1	2.3	1.9	1.3	0.6
Proximal end heating with bared-end treatment	4.2	3.4	1.9	4.3	3.3	0.9	0.7	0.5	0.2
Distal end heating with capped end treatment	28.3	25.2	16.1	23.7	20.9	12.5	0.1	0.1	0.1

Table 2. Measured temperature (°C) in medium 0.2 S/m.

	S1	S2	S3	L1	L2	L3	U1	U2	U3
Distal end heating with bared-end treatment	21.1	17.5	8.5	18.1	15.1	8.4	1.6	1.5	0.5
Proximal end heating with bared-end treatment	13.9	10.1	7.4	13.0	11.2	7.3	0.8	0.6	0.3
Distal end heating with capped end treatment	58.9	50.7	36.2	40.3	35.3	23.4	0.6	0.3	0.2

Using the measured data and the unscaled transfer function model developed based on the reciprocity method, the magnitude of transfer function models for the four configurations are given in Fig. 3(a) inside 0.47 S/m testing medium. For comparison, the transfer function models for the intact DBS system are also given in the figure. Similarly, the phases of the transfer function models are given in Fig. 3 (b). The TF models in medium 0.20 S/m are given in Fig. 3 (c)-(d).

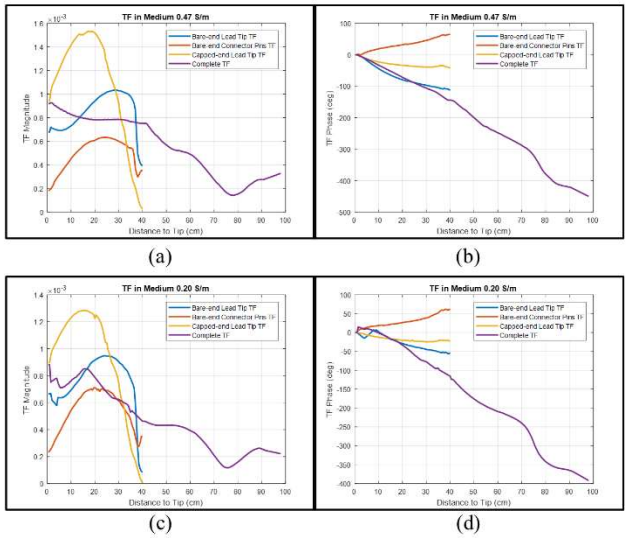

Fig. 3. The (a) magnitude and (b) phase of the TF in medium 0.47 S/m and the (c) magnitude and (d) phase of the TF in medium 0.2 S/m

The in-vivo RF-induced heating of all configurations (intact DBS system, abandoned leads with capped-end treatment, and abounded leads with bared-end treatment) is further evaluated with tangential electric fields along the trajectories and TFs in 0.47 S/m and 0.2 S/m. In addition, the RF-induced heating was evaluated at 21 imaging landmarks ranging from head image landmark to chest image landmark. For each landmark and TF, the RF-induced heating along 12600 implantation pathways are calculated. The RF-induced heating results are shown in Fig. 4. The upper and lower limits are the maximum and average values for each landmark. The circle dots are corresponding to the 95th percentile value of the RF-induced heating. It is shown that the maximum temperature rise at the lead tip with the

capped-end treatment is higher than the other two abandoned leads configurations. The temperature rise at proximal end of the abandoned leads end is smaller than the other two configurations.

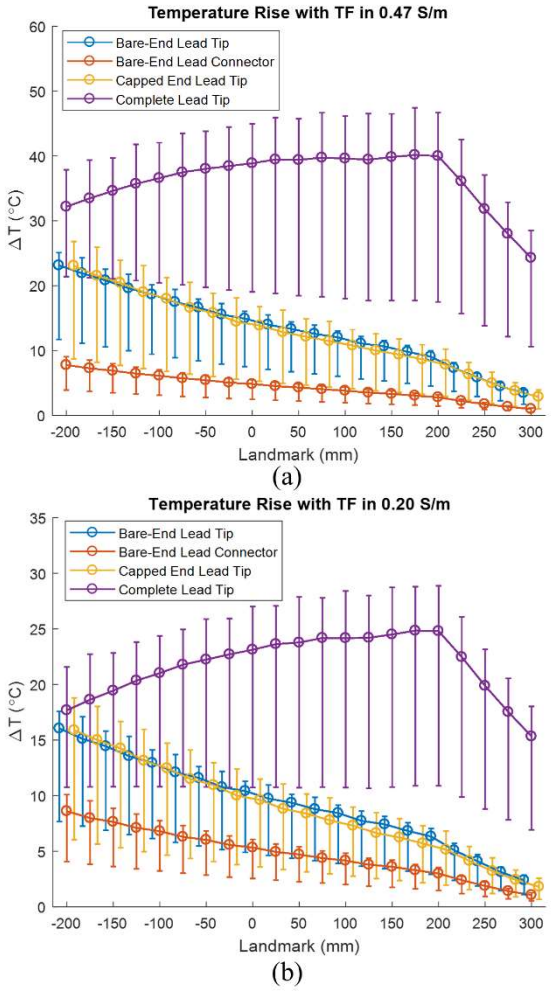

Fig. 4. The in-vivo RF-induced heating results at each landmark position with TFs in medium (a) 0.47 S/m and (b) 0.2 S/m.

The relative relationship for *in-vivo* RF-induced heating results is different from that measured inside the ASTM phantom. The measured temperature rise in phantom at the lead tip with the capped-end treatment is significantly higher than that with bared-end for the measurement results, while this difference is much smaller in the human body. The phase distribution of the TF is the main reason for this difference. The phase variation of the electric fields along the trajectories inside the human body can be more than 360 degrees, while the phase variation of the electric fields along the straight pathways inside the ASTM phantom is small at 1.5T (less than 45 degrees). Therefore, for the same transfer function models, the out-of-phase cancellation for electric fields along the implantation pathways inside human body model would generate to lower RF-induced heating as compared to that from the ASTM phantom measurements.

IV. Conclusion

The RF-induced heating of an abandoned leads from a commercial DBS system with either bared-end or capped-end treatment at the proximal end is evaluated in this study. The insulated abandoned DBS lead can have almost twice the temperature rise than the one with bared-end configuration in the ASTM phantom study, while this difference is reduced for the *in-vivo* evaluation. The maximum difference for the highest temperature rise at the lead tip with different treatments is lower. It is shown that the RF-induced heating behaviors of abandoned leads depend on the termination condition of the connector and the lead trajectories.

Disclaimer

The mention of commercial products, their sources, or their use in connection with material reported herein is not to be construed as either an actual or suggested endorsement of such products by the Department of Health and Human Services.

References

[1] S. Feng, R. Qiang, W. Kainz and J. Chen, "A Technique to Evaluate MRI-Induced Electric Fields at the Ends of Practical Implanted Lead," in *IEEE Transactions on Microwave Theory and Techniques*, vol. 63, no. 1, pp. 305-313, Jan. 2015

[2] *ISO/TS 10974:2018 Assessment of the Safety of Magnetic Resonance Imaging for Patients With an Active Implantable Medical Device. International Organization for Standardization*; 2018.

[3] Wang, R. Guo, W. Hu, J. Zheng, Q. Wang, J. Jiang, K. K. N. Kurpad, N. Kaula, S. Long, J. Chen, and W. Kainz, "Magnetic resonance conditionality of abandoned leads from active implantable medical devices at 1.5 T," *Magn. Reson. Med.*, vol. 87, no. 1, pp. 394–408, Jan. 2021.

[4] E. Mattei, G. Gentili, F. Censi, M. Triventi, G. Calcagnini, "Impact of capped and uncapped abandoned leads on the heating of an MR-conditional pacemaker implant," *Magn. Reson. Med.*, vol. 73, no. 1, pp, 390-400, Jan. 2015

[5] R. Guo, J. Zheng, Z. Wang, R. Yang, J. Chen and T. Hoegh, "Reducing the Radiofrequency-Induced Heating of Active Implantable Medical Device with Load Impedance Modification," *2020 IEEE International Symposium on Antennas and Propagation and North American Radio Science Meeting*, 2020, pp. 1487-1488

[6] *ASTM F 2182-19e2. Standard Test Method for Measurement of Radiofrequency Induced Heating near Passive Implants during Magnetic Resonance Imaging*. ASTM Committee F04 on Medical and Surgical Materials and Devices, Subcommittee F04.15 on Material Test Methods. ASTM International; 2019.

[7] A. Christ, W. Kainz, E. G. Hahn, K. Honegger, M. Zefferer, E. Neufeld, et al., "The virtual family—Development of surface-based anatomical models of two adults and two children for dosimetric simulations", *Phys. Med. Biol.*, vol. 55, no. 2, pp. N23-N38, Jan. 2010.